CHEMISTRY OF MATERIALS
Article

Chem. Mater. **2009,** *21,* 4241–4247 4241
DOI:10.1021/cm901224u

Electrochemically Template-Grown Multi-Segmented Gold-Conducting Polymer Nanowires with Tunable Electronic Behavior

Vincent Callegari,[†] Loïk Gence,[‡] Sorin Melinte,[‡] and Sophie Demoustier-Champagne*[,†]

[†]*Unité de Chimie et de Physique des Hauts Polymères (POLY), Université catholique de Louvain (UCL) Place Croix du Sud, 1, Louvain-la-Neuve 1348, Belgium, and* [‡]*Microelectronics Laboratory (DICE), Université catholique de Louvain (UCL) Place du Levant, 3, Louvain-la-Neuve 1348, Belgium*

Received May 4, 2009. Revised Manuscript Received August 6, 2009

Multisegmented nanowires (NWs) based on poly(3,4-ethylenedioxythiophene) (PEDOT) and polypyrrole (PPy) are synthesized by an all-electrochemical template method for precise control over segment dimensions. We study the influence of different parameters on the growing process of the PEDOT segment and on the mechanical strength of the conjugated polymer/metal interfaces in tri-segmented Au-PEDOT-Au and tetra-segmented Au-PEDOT-PPy-Au NWs. The coexistence of PEDOT and PPy in tetra-segmented NWs is confirmed by high resolution transmission electron microscopy coupled with energy-dispersive X-ray analysis. We investigate the electrical transport of individual multisegmented NWs of both types at room temperature. An interesting feature of the tetra-segmented NWs compared to tri-segmented NWs is the switching of their electrical characteristics in function of the redox state of the two conjugated polymer blocks.

Introduction

Nanojunctions (metal/molecules or nanoparticles/metal) are of great interest both for improving our fundamental understanding of electrical transport at the nanoscale and for the technological development of novel electronic devices.[1] Impressive progress has been made on carbon nanotubes[2] and low molecular weight organic molecules including alkanethiol monolayers, dithiols, and conjugated oligomers.[3] However, fewer reports[4] dealt with the fabrication of nanojunctions by using conducting or semiconducting polymers, though the outstanding opto-electronic properties of conjugated polymers, such as their reversible modulation from metals to insulators by tuning the dopant concentration levels, have been well-known for more than 20 years.[5]

To date, conductive polymer nanotubes and nanowires have been fabricated by various methods[6] that can be divided in three categories: hard template,[7] soft template,[8] and template-free methods.[9] Though all of these methods are commonly used to fabricate one-component systems, only the hard template method offers the ability to generate multicomponent nanowires—made from organic and inorganic materials—with a very good control over the composition and spatial distribution of the different nanowire blocks.[10] On the basis of this template-based strategy, we have developed an all-electrochemical process, consisting in the sequential deposition of metallic and conjugated polymer segments within the pores of polycarbonate membranes.[11] A major advantage of this all-electrochemical method compared to chemical processes is that it provides excellent control over the

*To whom correspondence should be addressed. Tel.: +32-10-472702. Fax: +32-10-451593. E-mail: sophie.demoustier@uclouvain.be.

(1) For reviews see (a) Lindsay, S. M.; Ratner, M. A. *Adv. Mater.* **2007**, *19*, 23. (b) Selzer, Y.; Allara, D. *Annu. Rev. Phys. Chem.* **2006**, *57*, 593. (c) Nitzan, A.; Ratner, M. A. *Science* **2003**, *300*, 1384. (d) Joachim, C.; Glimzewski, J. K.; Aviram, A. *Nature* **2000**, *408*, 541.
(2) (a) Baughman, R. H.; Zakhidov, A. A.; de Heer, W. A. *Science* **2002**, *297*, 787. (b) Nitzan, A.; Ratner, M. A. *Science* **2003**, *300*, 1384.
(3) (a) Holmlin, R. E.; Haag, R.; Chabinyc, M. L.; Ismaligov, R. F.; Cohen, A. E.; Terfort, A.; Rampi, M. A.; Whitesides, G. M. *J. Am. Chem. Soc.* **2001**, *123*, 5075. (b) Wold, D. J.; Frisbie, C. D. *J. Am. Chem. Soc.* **2001**, *123*, 5549. (c) James, D. K.; Tour, J. M. *Chem. Mater.* **2004**, *16*, 4423. (d) McCreery, R. L. *Chem. Mater.* **2004**, *16*, 4477. (e) Akkerman, H. B.; Blom, P. W. M.; de Leew, D. M.; de Boer, B. *Nature* **2006**, *441*, 69. (f) Van Hal, P. A.; Smits, E. C. P.; Geuns, T. C. T.; Akkerman, H. B.; De Brito, B. C.; Perissinotto, S.; Lanzani, G.; Kronemeijer, A. J.; Geskin, V.; Cornil, J.; Blom, P. M. W.; De Boer, B.; De Leeuw, D. M. *Nat. Nanotechnol.* **2008**, *3*, 749.
(4) (a) Zhao, J. H.; Thomson, D. J.; Pillai, R. G.; Freund, M. S. *Appl. Phys. Lett.* **2009**, *94*, 092113. (b) Barman, S.; Deng, F.; McCreery, R. L. *J. Am. Chem. Soc.* **2008**, *130*, 11073.
(5) (a) Brédas, J. L.; Scott, B. J.C.; Yakushi, K.; Street, G. B. *Phys. Rev. B* **1984**, *30*, 1023. (b) Chiang, J. C.; MacDiarmid, A. G. *Synth. Met.* **1986**, *13*, 193. (c) Epstein, A. J.; Ginder, J. M.; Zuo, F.; Bigelow, R. W.; Woo, H. S.; Tanner, D. B.; Richter, A. F.; Huang, W. S.; MacDiarmid, A. G. *Synth. Met.* **1987**, *18*, 303. (d) Yoon, C. O.; Reghu, M.; Moses, D.; Heeger, A. J. *Phys. Rev. B* **1994**, *49*, 10851.
(6) (a) For recent reviews see: Jang, J. *Adv. Polym. Sci.* **2006**, *199*, 189. (b) Yoon, H. S.; Choi, M. J.; Lee, K. A.; Jang, J. S. *Macromol. Res.* **2008**, *16*, 85.
(7) (a) Martin, C. R. *Adv. Mater.* **1991**, *3*, 457. (b) Martin, C. R. *Acc. Chem. Res.* **1995**, *28*, 61. (c) Martin, C. R. *Chem. Mater.* **1996**, *8*, 1739. (d) Duchet, J.; Legras, R.; Demoustier-Champagne, S. *Synth. Met.* **1998**, *98*, 113. (e) Demoustier-Champagne, S.; Stavaux, P. Y. *Chem. Mater.* **1999**, *11*, 829.
(8) Wie, Z. X.; Wan, M. X.; Lin, T.; Dai, L. M. *Adv. Mater.* **2003**, *15*, 136.
(9) (a) Huang, J.; Virji, S.; Weiller, B. H.; Kaner, R. B. *Chem.—Eur. J.* **2004**, *10*, 1314. (b) Zang, J. F.; Li, C. M.; Bao, S. J.; Cui, X. Q.; Bao, Q. L.; Sun, C. Q. *Macromolecules* **2008**, *41*, 7053.
(10) (a) Kovtyukhova, N. I.; Mallouk, T. E. *Chem.—Eur. J.* **2002**, *8*, 4355. (b) Hurst, S. J.; Payne, E. K.; Qin, L.; Mirkin, C. A. *Angew. Chem., Int. Ed.* **2006**, *45*, 2672.
(11) Reynes, O.; Demoustier-Champagne, S. *J. Electrochem. Soc.* **2005**, *152*, D130.

Published on Web 08/25/2009

length of each nanowire segment, simply by adjusting the amount of charge passed through the system. In our previous works,[12] we reported on the synthesis and structural characterization of narrow (40 to 90 nm in diameter) multisegmented metal (Au or Pt)/polypyrrole (PPy) nanowires. The study of their electrical properties by variable temperature transport measurements revealed that both multiple and single nanowires exhibit symmetrical current−voltage characteristics and no rectification effect.

Recently, with the aim of studying systems with multimolecular components, we adapted the template method for preparing novel hybrid metal/conjugated polymer nanowires (NWs). For the development of nanoscale electronic devices, poly(3,4-ethylenedioxythiophene) (PEDOT) exhibits a number of desirable properties in the oxidized state, including high conductivity and excellent environmental stability.[13] In this respect, special attention was paid to the optimization of PEDOT-based nanowire synthesis. Herein, we present a highly reproducible route based upon the electrochemical template-based strategy for preparing well-shaped and mechanically robust tri-segmented Au-PEDOT-Au and tetra-segmented Au-PEDOT-PPy-Au NWs. Remarkably, the tetra-segmented NWs switch their electrical characteristics as a function of the redox state of the conjugated polymer blocks.

Experimental Section

Materials. Polycarbonate track-etched membranes with a thickness of 21 μm, a pore density of 10^9 pores$\cdot$cm^{-2}, and an average pore size of 60 or 110 nm, supplied by it$_4$ip s.a.,[14] were used as nanoporous templates. Pyrrole (Acros, 99%) was purified immediately before use by passing it through a microcolumn constructed from a Pasteur pipet, glass wool, and activated alumina. The 3,4-ethylenedioxythiophene (EDOT, Sigma-Aldrich), lithium perchlorate ($LiClO_4$, Acros), potassium chloride (KCl, Acros), potassium hydrogenophosphate (K_2HPO_4, Acros), hydrogen tetrachloroaurate ($HAuCl_4$, Sigma Aldrich, 99,9%), and dichloromethane (CH_2Cl_2, Acros) were used without any prior purification. Deionized water was used to prepare all aqueous solutions. Aqua regia was prepared by carefully adding three volumes of concentrated hydrochloric acid (HCl, Acros) to one volume of concentrated nitric acid (HNO_3, Acros, 63%). ***Caution!*** Aqua regia solution is a strong oxidizing agent.

Preparation of Tri-Segmented Au-PEDOT-Au Nanowires. All electrochemical experiments were performed with a CHI660B Electrochemical Workstation (CH Inc.) in a conventional one-compartment cell at room temperature with a Pt disk counter-electrode and a Ag/AgCl reference electrode. A 500 nm thick layer of gold evaporated on one side of the polycarbonate membrane served as the working electrode. Electrodeposition of Au was performed by cycling the potential of the working electrode from 0.7 to 0 V at 200 mV$\cdot$s^{-1} using a homemade cyanide free solution (0.1 M KCl, 0.1 M K_2HPO_4, and 0.03 M $HAuCl_4$ in deionized water). Electropolymerization of EDOT was carried out by cyclic voltammetry from an aqueous solution containing 0.1 M $LiClO_4$ and various monomer concentrations ranging from 1 to 14 mM. The potential was swept between 0.2 V and different upper potential limits ($0.85 \leq$ UPL ≤ 1.1 V) with scan rates ranging from 200 to 800 mV$\cdot$s^{-1}.

Preparation of Tetra-Segmented Au-PEDOT-PPy-Au Nanowires. Electrodeposition of the bottom and top Au segments was performed by cycling the potential of the working electrode from 0.7 to 0 V at 200 mV$\cdot$s^{-1} using a homemade cyanide free solution (0.1 M KCl, 0.1 M K_2HPO_4, and 0.03 M $HAuCl_4$ in deionized water). The electrosynthesis of the PEDOT was carried out by cyclic voltammetry from an aqueous solution containing 14 mM of EDOT and 0.1 M $LiClO_4$. The potential was swept between 0.2 to 1.1 V at a scan of 400 mV$\cdot$s^{-1}. Electropolymerization of pyrrole was performed in deionized water in the presence of 0.1 M $LiClO_4$ and 0.02 M pyrrole, by sweeping the potential between 0 and 0.85 V at a scan rate of 400 mV$\cdot$s^{-1}.

Structural Analysis. The dimensions and morphology of the nanowires were studied by scanning electron microscopy (SEM) and by transmission electron microscopy (TEM) after dissolution of the PC template. SEM pictures were obtained using a LEO 982 field emission scanning electron microscope (FE-SEM, Carl Zeiss SMT Inc.) at an accelerating voltage of 1 kV. TEM pictures were obtained using a LEO 922 transmission electron microscope (Carl Zeiss SMT Inc.) operating at 200 kV. After removing the evaporated metal layer with aqua regia and dissolving the template in dichloromethane, two or three drops of the resulting nanowire suspension were placed on a carbon film grid (Agar Scientific Ltd.). Energy dispersive X-ray spectroscopy (EDX) experiments were carried out with the LEO 922 TEM equipped with an INCA x-sight detector (Oxford Instruments).

Electrical Characterization. Single nanowires were measured by a top contact approach briefly described below. After the dissolution of the PC membrane, the nanowires were dispersed in dichloromethane. This solution was dropped onto an oxidized silicon substrate prepared with thick Cr/Au pads defined by photolithography. After drying the solution, the nanowires remain attached to the substrate surface via van der Waals forces; optical and electron microscopy were used to determine the position of isolated nanowires. Nanosized Au electrical probes were subsequently deposited by electron beam lithography (EBL) and lift-off for each nanowire; the probes were defined specifically to fit to the Cr/Au pads design. Prior to the deposition of the Au electrodes, a short cleaning oxygen plasma was performed to remove all PC and resist residues that could remain on the NWs due to the previous processing steps. This ensures a clean nanowire-to-electrode interface, which translates into a good electrical contact. Electrical measurements were performed with an Agilent B1500 semiconductor parameter/device analyzer equipped with high current resolution ($\sim$0.1 fA) source measure units and a Süss-Microtech Probe Station. No measurable leak currents have been observed through the oxide layer or between nonconnected pads over the voltage range scanned in the experiments.

Results and discussion

Growth and Morphological Analysis of Au-PEDOT-Au Tri-Segmented Nanowires. We have carried out a systematic study of the electrochemical growth, by cyclic

(12) (a) Gence, L.; Faniel, S.; Gustin, C.; Melinte, S.; Bayot, V.; Callegari, V.; Reynes, O.; Demoustier-Champagne, S. *Phys. Rev. B* **2007**, *76*, 115415. (b) Gence, L.; Callegari, V.; Faniel, S.; Vlad, A.; Dutu, C.; Melinte, S.; Demoustier-Champagne, S.; Bayot, V. *Phys. Status Solidi A* **2008**, *205*, 1447.

(13) (a) Pei, Q. B.; Zuccarello, G.; Ahlskog, M.; Inganas, O. *Polymer* **1994**, *35*, 1347. (b) Groenendaal, L. B.; Jonas, F.; Freitag, D.; Pielartzik, H.; Reynolds, J. R. *Adv. Mater.* **2000**, *12*, 481. (c) Groenendaal, L.; Zotti, G.; Aubert, P. H.; Reynolds, J. R. *Adv. Mater.* **2003**, *15*, 855. (d) Kirchmeyer, S.; Reuter, K. *J. Mater. Chem.* **2005**, *15*, 2077.

(14) http://www.it4ip.be/.

Table 1. Electropolymerization Conditions Used in This Study for the Synthesis of the PEDOT Nanowire Segment

entry	concentration (mM)	potential scan range (V)	scan rate ($mV \cdot s^{-1}$)	scans (no.)
1	14	0.2−0.85	400	1000
2	14	0.2−0.9	400	1000
3	14	0.2−1.0	400	1000
4	14	0.2−1.1	400	1000
5	1	0.2−1.1	400	1000
6	5	0.2−1.1	400	500
7	14	0.2−1.1	400	200
8	14	0.2−1.1	200	200
9	14	0.2−1.1	800	200

voltammetry, of hybrid NWs containing PEDOT junctions in polycarbonate membranes. As the mechanical properties of the hybrid nanowires are key for their use as individually addressable electronic components, the effect of several parameters such as the monomer concentration, the potential scan range, and the scan rate on the morphology and the strength of the metal/polymer interfaces of the resulting tri-segmented nanowires was investigated by SEM and TEM (see Experimental Section). The major results of this study are summarized in Table 1. The value of the applied potential is one of the most significant parameters in an electropolymerization process. Therefore, experiments to establish the highest and lowest potential values at which it is possible to obtain well-shaped PEDOT nanowires were first carried out. The upper potential value is conditioned by the fact that the polymer has not to be overoxidized. On the basis of the work of Du et al.,[15] we thus decided to select potentials lower than 1.1 V.

The 3,4-ethylenedioxythiophene (EDOT) was electropolymerized, from an aqueous solution containing 0.1 M $LiClO_4$ and 14 mM EDOT, by sweeping the potential between 0.2 V and various upper potentials 0.85, 0.9, 1.0, and 1.1 V (Table 1, entries 1−4). Figure 1 shows typical TEM pictures of the nanowires obtained under these four different electrosynthesis conditions. By sweeping the potential to an upper value less than 0.9 V, a very small amount of PEDOT (segment length ≤ 40 nm) is formed on the bottom gold segment, even after 1000 scans (Figure 1a), and no top metal segment can be grown further. Sweeping the potential to higher upper values—from 0.9 to 1.1 V—allowed the subsequent deposition of Au segments and, hence, led to the formation of entire Au-PEDOT-Au NWs (Figure 1b−d), with PEDOT junctions of increasing length. Moreover, for these three upper potential limits, the polymer segment is dense on its whole length. For the upper potential limit of 1.1 V, the polymer/metal interfaces appear stronger, as only less than 25% of the tri-segmented NWs are broken when freed from the template, while the percentage of broken NWs is around 50% for upper potential limits of 0.9 and 1.0 V.

For that reason, we further carry out EDOT electropolymerization using a fixed potential window from 0.2 to 1.1 V. As EDOT is poorly soluble in aqueous solutions, low enough concentrations, ranging from 1 to 14 mM, were used to guarantee homogeneous media. When using an EDOT concentration equal to 1 mM (Table 1, entry 5), no polymer is formed even after a large number of potential scans. By increasing the monomer concentration (Table 1, entries 4 and 6), we fabricate high-quality PEDOT segments. Accordingly, the PEDOT growth is approximately 3 times faster when the monomer concentration is increased from 5 to 14 mM.

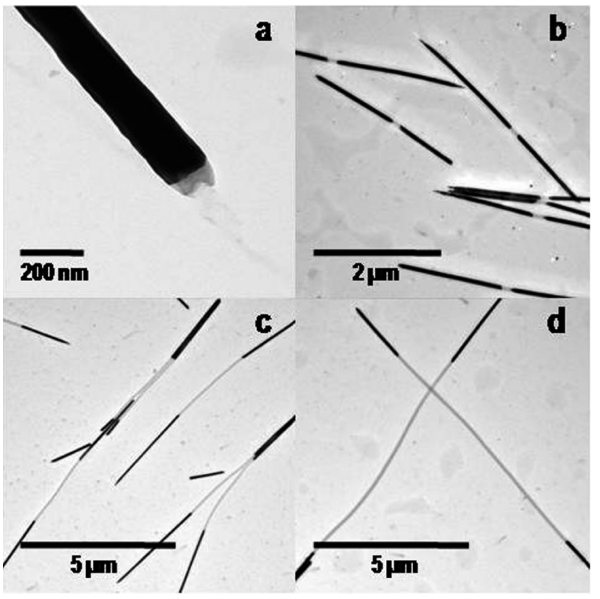

Figure 1. TEM images of PEDOT-based nanowires, where the polymer was synthesized using different upper potential limits: (a) 0.85 V, (b) 0.9 V, (c) 1 V, and (d) 1.1 V.

Then, EDOT was electropolymerized from an aqueous solution of 0.1 M $LiClO_4$ and 14 mM EDOT by sweeping the potential between 0.2 and 1.1 V at different scan rates: 200, 400, and 800 $mV \cdot s^{-1}$ (Table 1, entries 7−9). As shown by the TEM pictures (Figure 2), the potential scan rate has a huge impact on the shape of the Au-onto-PEDOT interface. Indeed, at low scan rate (200 $mV \cdot s^{-1}$), a very long meniscus is formed at the end of the PEDOT nanowire segment. The very thin walls of this PEDOT tubular part are too fragile to strongly maintain the top metal segment, resulting in a high percentage of broken nanowires. When applying a fast scan rate (800 $mV \cdot s^{-1}$), flat Au-onto-PEDOT interfaces are obtained that also present a very low mechanical strength. Interestingly, at an intermediate scan rate of 400 $mV \cdot s^{-1}$, a conical short gold meniscus soaring into the PEDOT junction is observed, ensuring a strong mechanical link between the polymer and the top metal section. The different top structures observed for the PEDOT segment (ranging from tubular to full-nanowire structures) as a function of the electrochemical growing rate, are in good agreement with the electrochemical synthetic mechanism of PEDOT nanotube and nanowire formation, recently reported by Lee et al.[16]

Finally, to calibrate the growth of the PEDOT segment, EDOT electropolymerization was carried out, under the

(15) Du, X.; Wang, Z. *Electrochim. Acta* **2003**, *48*, 1713.

(16) (a) Xiao, R.; Cho, S. I.; Liu, R.; Lee, S. B. *J. Am. Chem. Soc.* **2007**, *129*, 4483. (b) Cho, S. I.; Lee, S. B. *Acc. Chem. Res.* **2008**, *41*, 699.

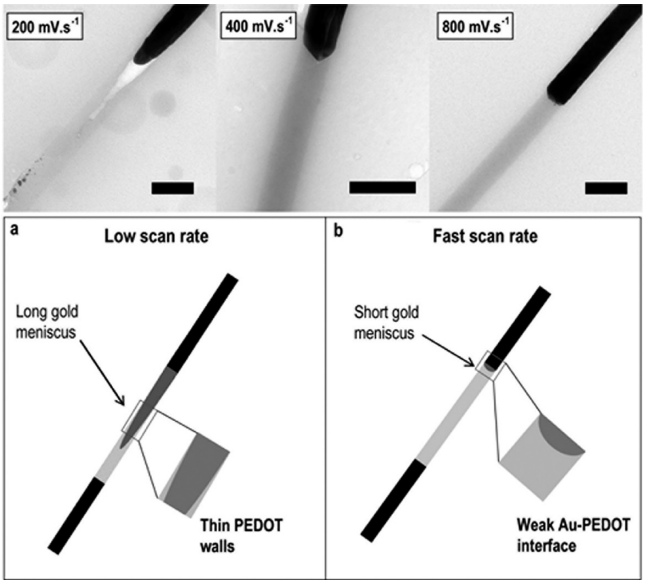

Figure 2. (Top) TEM pictures showing the different morphologies of the Au-onto-PEDOT interface depending on the potential scan rates. Scale bars: 200 nm. (Bottom) Scheme illustrating the shape of the Au-onto-PEDOT interface: (a) at slow potential scan rate and (b) at fast potential scan rate.

optimized conditions (14 mM concentration, 0.2 to 1.1 V scanning potential, and 400 $mV \cdot s^{-1}$ scanning rate), for different scan numbers. SEM micrographs (Figure 3a,b) show that Au-PEDOT-Au nanowires can be grown with various polymer junction lengths and can then be removed intact from the template.

Figure 3c shows the evolution of the PEDOT segment length as a function of the number of cyclic voltammetric scans. Each point in the plot was obtained by averaging the lengths of approximately 100 nanowires in TEM images. We observed a linear dependence of the average length of the PEDOT segment on the number of scans, with a mean growth rate of 10 nm/scan, below 500 voltammetric cycles. Then, for longer deposition periods, the PEDOT growth rate slightly decreases (8 nm/scan), probably due to a slight increase of the resistivity of very long PEDOT segments. It should however be pointed out that very long PEDOT junction ($>15\ \mu m$) can be prepared, while electrode passivation occurred rather earlier with PPy, where the longest electropolymerizable polymer junction was $\sim 3\ \mu m$.[11]

Electrical Characterization of Au-PEDOT-Au Nanowires. We performed the electrical characterization of single tri-segmented Au-PEDOT-Au nanowires (NWs) at room temperature (see Experimental Section). Here, we present results for three samples (NW1, NW2, and NW3) with diameter of 110 nm and PEDOT segment lengths of 0.6, 1.2, and 4.5 μm, respectively. For the two-point measurements, the measured resistances also include an unavoidable contact resistance R_c in series with the tri-segmented nanowires. From measurements of gold nanowires (see lower inset of Figure 6) we deduce that $R_c < 10^2\ \Omega$, which is negligible compared to the resistance of the polymer segments ($\sim 10^8\ \Omega$). The two-point current−voltage ($I-V$) characteristics of the samples NW1 and NW2 are given in Figure 4 (top panel) together with the two-point $I-V$ characteristic of sample NW3 (outer

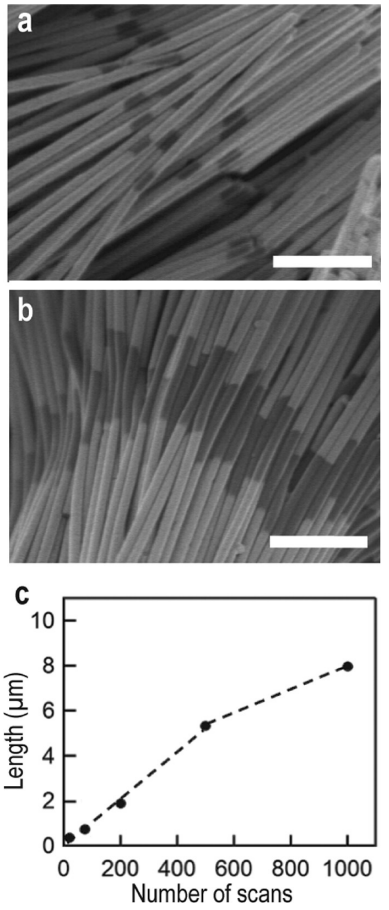

Figure 3. SEM pictures of 110 nm diameter tri-segmented Au-PEDOT-Au nanowires presenting two different polymer junction lengths: (a) 200 nm (20 scans) and (b) 1 μm (100 scans). The good contrast between the metallic and the polymer segments on SEM pictures allows for growth calibration. Scale bars: 1 μm. (c) Length of the PEDOT segment as a function of the number of potential scans between 0.2 and 1.1 V.

contacts, see bottom inset to Figure 4). All samples exhibit symmetrical and linear $I-V$ characteristics, consistent with Ohmic contacts between the PEDOT and the gold segments.[17,18] Room-temperature conductivities of 4.3, 2.5, and 450 $mS \cdot cm^{-1}$ were deduced from the slopes of the $I-V$ curves. The rather large variability of the conductivity in the as-synthesized samples is unavoidable due to the postsynthesis processing, including the number and the position of the contacts (see Supporting Information). In particular, since nanowire-based field effect transistors are intensely scrutinized for elucidating the charge transport mechanisms at nanoscale in organic semiconductors,[19−24] the samples have been investigated

(17) Cao, Y.; Kovalev, A. E.; Xiao, R.; Kim, J.; Mayer, T. S.; Mallouk, T. E. *Nano Lett.* **2008**, *8*, 4653.
(18) Duvail, J. L.; Long, Y.; Cuenot, S.; Chen, Z.; Gu, C. *Appl. Phys. Lett.* **2007**, *90*, 102114.
(19) Pinto, N. J.; Johnson, A. T.; MacDiarmid, A. G.; Mueller, C. H.; Theofylaktos, N.; Robinson, D. C.; Miranda, F. A. *Appl. Phys. Lett.* **2003**, *83*, 4244.
(20) Briseno, A. L.; Mannsfeld, S. C. B.; Jenekhe, S. A.; Bao, Z.; Xia, Y. *Mater. Today* **2008**, *11*, 38.
(21) Aleshin, A. N. *Adv. Mater.* **2006**, *18*, 17.
(22) Chung, H.-J.; Jung, H. J.; Cho, Y.-S.; Lee, S.; Ha, J.-H.; Choi, J. H.; Kuk, Y. *Appl. Phys. Lett.* **2005**, *86*, 213113.
(23) Hsu, F.-C.; Prigodin, V. N.; Epstein, A. J. *Phys. Rev. B* **2006**, *74*, 235219.
(24) Kim, B. H.; Park, D. H.; Joo, J.; Yu, S. G.; Lee, S. H. *Synth. Met.* **2005**, *150*, 279.

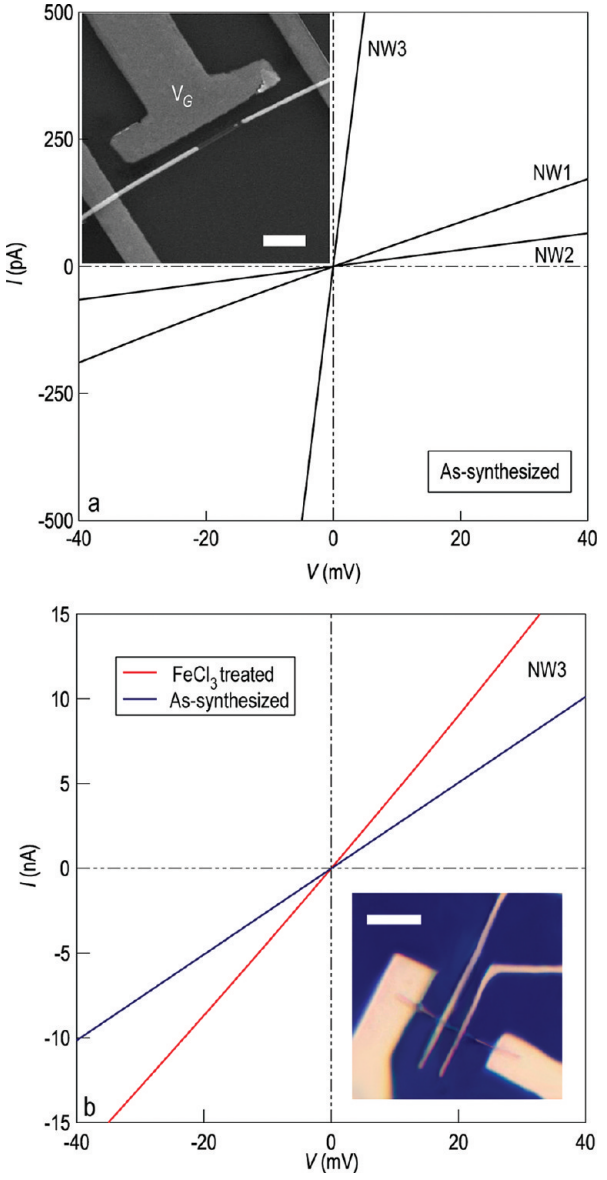

Figure 4. (Top) Two-point $I-V$ characteristics of tri-segmented Au-PEDOT-Au nanowires. The upper inset is a SEM picture of sample NW2. The scale bar is 1 μm. Four probes are contacting NW3; the outer contacts have been used for estimating its two-point resistance. (Bottom) Four-point $I-V$ characteristics of NW3 measured before (blue curve) and after (red curve) $FeCl_3$ treatment. The scale bar is 5 μm.

in side-gate and bottom-gate configurations (see Supporting Information). The interaction of PEDOT with electron acceptors causes variations in both carrier density and mobility, leading to significant changes in the conductivity. We performed a chemical oxidative treatment, by immersing the samples in a $FeCl_3$ 0.5 M solution for 1 h. As shown in Figure 4 (bottom panel), due to the shift in the dopant anion equilibrium within the PEDOT, we observe a conductivity increase of the polymer segment.

Growth of Au-PEDOT-PPy-Au Tetra-Segmented Nanowires. Tetra-segmented nanowires presenting a polymer heterojunction (PEDOT-PPy) were synthesized by the template sequential electrochemical deposition method. To get mechanically strong nanowires, the sequence of polymer deposition was determined according to previous observations on the shape and strength of the different metal−polymer interfaces. PEDOT was thus first deposited on the Au segment, as the strong chemical bond between Au−S compensates for the weakness of the flat, conjugated polymer-onto-metal bottom interface. PPy was then electrodeposited onto the PEDOT segment, the strength of the metal-onto-PPy interface being ensured by its meniscus shape.[12]

Morphological Analyses of Au-PEDOT-PPy-Au Nanowires. The formation of the PEDOT-PPy heterojunction within Au nanowires was confirmed by high-resolution TEM. Representative Au-PEDOT-PPy-Au nanowires, after removal of the polycarbonate template, are shown in Figure 5a,b.

A zoom into the PEDOT−PPy interface is presented in the inset of Figure 5a. On this picture, it appears that one of the two polymers shrank much more than the other one during solvent evaporation in a sampling process. To unambiguously distinguish the polymer segments, we employed energy-dispersive X-ray (EDX) analysis. Figure 5c shows EDX spectra recorded on the four spots marked in Figure 5b. These spectra reveal the presence of sulfur atoms, characteristic for PEDOT, only in the narrow nanowire segment. Therefore, two consecutive segments of PEDOT and PPy were synthesized, and the first one could be ascertained by its lower diameter.

Electrical Characterization of Au-PEDOT-PPy-Au Nanowires. Similar to tri-segmented NWs, we performed the electrical characterization of tetra-segmented NWs at room temperature. Figure 6 presents the symmetrical and linear $I-V$ characteristic of a single tetra-segmented Au-PEDOT-PPy-Au specimen. An interesting feature of the tetra-segmented NWs compared to tri-segmented NWs is provided by their ability to switch their electrical behavior as a function of the redox state of the two conjugated polymer blocks. Indeed, as shown in Figure 6, the resistance of the tetra-segmented sample in its as-synthesized state (blue curve) is much higher than that of samples NW1, NW2, and NW3. This could be attributed essentially to the PEDOT−PPy junction, as both PEDOT[17] and PPy[12] are known to form Ohmic contacts with gold. After a chemical oxidative treatment, performed by immersing the tetra-segmented sample in a $FeCl_3$ 0.5 M solution for 1 h, it exhibited a highly nonlinear $I-V$ characteristic (Figure 6, red curve), accompanied by a current increase.[24] Furthermore, the $I-V$ curve is asymmetric, and the gain of current depends on the sign of the bias voltage V. Roughly, the gain is enhanced by a factor of 2 at negative bias compared to positive bias. The chloride ions inserted during the chemical oxidative treatment effectively adjust the low-dimensional carrier hopping network on the backbone of the polymers inducing an enhanced charge transport.[23]

Finally, to explain the nonlinear behavior displayed by the Au-PEDOT-PPy-Au NWs after treatment with $FeCl_3$, we studied by X-ray photoelectron spectroscopy (XPS) the evolution of the electronic structure and doping ratio of PEDOT and PPy layers upon oxidative treatment (Supporting Information). When the electrosynthesized PEDOT and PPy were treated with 0.5 M $FeCl_3$ for 1 h, a

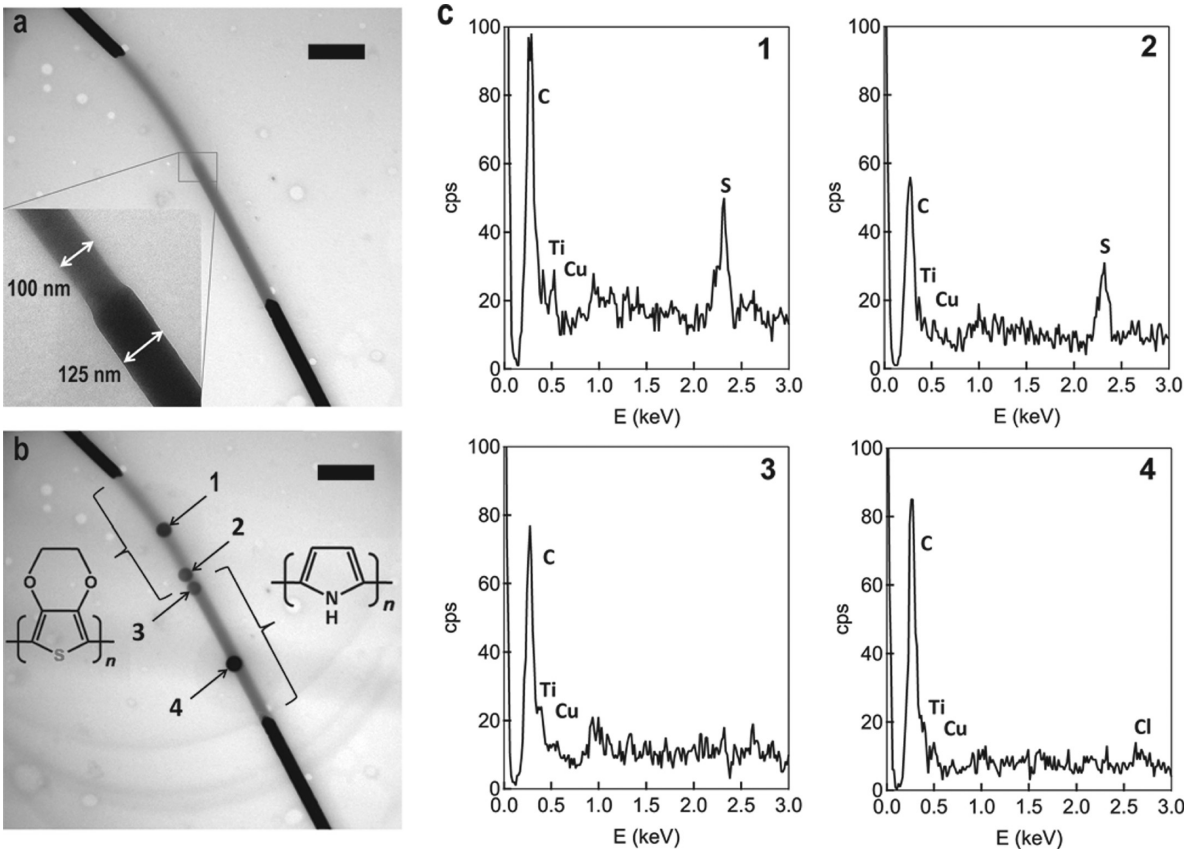

Figure 5. (a) TEM picture of a 110 nm diameter tetra-segmented Au-PEDOT-PPy-Au nanowire. The inset shows a zoom of the heterojunction. (b) TEM picture showing four analyzed areas marked by a dark spot corresponding to the polymer degradation by the electron beam. Scale bars: 500 nm. (c) EDX spectra recorded at the extremities of the two polymer segments. The carbon−copper grid and the titanium holder explain the presence of Cu and Ti peaks, respectively.

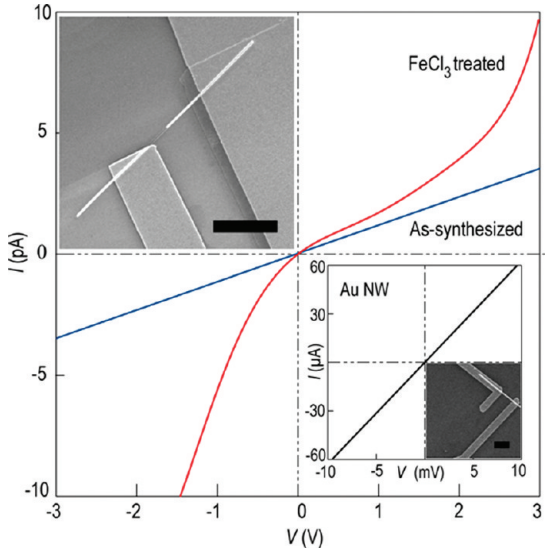

Figure 6. $I-V$ characteristics of a single tetra-segmented Au-PEDOT-PPy-Au nanowire measured before (blue curve) and after (red curve) $FeCl_3$ treatment. The upper inset is a SEM picture of a connected tetra-segmented nanowire. The scale bar is 10 μm. The lower inset shows the $I-V$ characteristic measured for the depicted single gold nanowire. The scale bar is 2 μm.

full exchange of counterions occurred in both types of polymers, the initial ClO_4^- anions being replaced by Cl^- species (Supporting Information, Figure S1). However, the electronic structure and the doping ratio of the PEDOT are only slightly dependent upon post-treatment (35% for the as-synthesized film and 32% for the $FeCl_3$-treated film; Supporting Information, Table S2), while the PPy is severely affected by $FeCl_3$ exposure. Indeed, overoxidation occurs in PPy, leading to the formation of imine-like (—N═) bonds (~16%) together with a significant decrease of the doping ratio (23%) for the as-synthesized film and 15% for the $FeCl_3$-treated film (Supporting Information, Table S3).

Conclusions

In this work, we present an effective all-electrochemical template-based method for preparing well-shaped and mechanically robust tri-segmented Au-PEDOT-Au and tetra-segmented Au-PEDOT-PPy-Au nanowires. Our systematic study of the influence of several parameters (monomer concentration, potential scan range, and scan rate) on the electropolymerization process of PEDOT in nanoporous polycarbonate membrane reveals that the morphology and the strength of the metal/polymer interfaces can be tuned by playing on the conducting polymer growth rate. The electrical properties at room temperature of individual multisegmented NWs were investigated. While the tri-segmented NWs exhibit symmetrical and linear $I-V$ characteristics, the tetra-segmented NWs switch to nonlinear electrical behavior by exposure to $FeCl_3$. As shown by XPS, this can be attributed to the

selective overoxidation of the PPy segment, leading to strong modifications of its electronic structure and doping ratio. Of course, the highly reproducible synthetic procedure described here can be exploited for producing other novel conjugated polymer-based multisegmented nanowires with desirable electrical properties. These structures could be useful for a wide range of electronic and sensor devices, and efforts to explore these opportunities are underway.

Acknowledgment. We thank Etienne Ferain and it_4ip company for supplying polycarbonate membranes and Michel Genet for helpful discussions about the XPS results. The work was supported by the Communauté française de Belgique (Action de recherche concertée, NANOMOL), by the Belgian Science Policy through the Interuniversity Attraction Pole Programs (P6/27 and P6/42), and by the Wallonia Region (NANOTIC program). S.D.C. and S.M. thank the F.R.S.-FNRS for their Senior Research Associate and Research Associate positions.

Supporting Information Available: XPS spectra showing the evolution of the electronic structure and doping ratio of PEDOT and PPy layers upon oxidative treatment by $FeCl_3$ and the results on three-terminal measurements of tri-segmented nanowires (PDF). This material is available free of charge via the Internet at http://pubs.acs.org.